Supporting Information

Copper(II)-Thymine Coordination Polymer Nanoribbons as Potential Oligonucleotide Nanocarriers

Verónica G. Vegas, Romina Lorca, Ana Latorre, Khaled Hassanein, Carlos J. Gómez-García, Oscar Castillo, Álvaro Somoza,* Félix Zamora,* and Pilar Amo-Ochoa*

S1. Materials and Methods

All reagents and solvents were purchased from standard chemical suppliers and used as received. IR spectra were recorded on a PerkinElmer 100 spectrophotometer using a PIKE Technologies MIRacle Single Reflection Horizontal ATR Accessory from 4000-600 cm^{-1}. Elemental analyses were performed on an LECO CHNS-932 Elemental Analyzer. Powder X-ray diffraction have been collected using a Diffractometer PANalyticalX'Pert PRO θ/2θ primary monochromator and detector with fast X'Celerator. The samples have been analysed with scanning θ/2θ.

Direct Current (DC) electrical conductivity measurements were carried out on different single crystals of compound **1** with graphite paste at 300 K and two contacts. The contacts were made with wolframium wires (25 μm diameter). The samples were measured at 300 K applying an electrical current with voltages form +10 to -10 V.

Magnetic measurements were done in a Quantum Design MPMS-XL-5 SQUID magnetometer in the 2-300 K temperature range with an applied magnetic field of 0.1 T on a polycrystalline sample of compound **1** and on a sample formed by nano-ribbons (**1n**) (with masses of 4.73 and 14.64 mg, respectively). Additionally, we measured the nano-ribbons (0.54 mg) in a water suspension and also in dry after removing the water. The susceptibility data were corrected for the sample holders previously measured under the same conditions, and for the diamagnetic contributions as deduced by using Pascal´s constant Tables (χ_{dia}= -310.1x10^{-6} emu.mol^{-1} for **1**).[1] The Hamiltonianis written as:

$$H = -J\sum_i S_i \cdot S_{i+1}$$

solid line in Figure 2G.

Atomic Force Microscope (AFM) images were acquired in dynamic mode using a Nanotec Electronica system (www.nanotec.es) operating at room temperature in ambient air conditions. For AFM measurements, Olympus cantilevers were used with a nominal force constant of 0.75 N/m and a resonance frequency of about 70 kHz. The images were processed using WSxM. The surfaces used for AFM were SiO_2 300 nm thickness (IMS Company). SiO_2 surfaces were sonicated in ultrasound bath at 37 Khz and 380 Watts, for 15 min in acetone, 15 min in 2-propanol and then dried under an Argon flow. *AFM Sample preparation.* Diluted suspension of compound **1n** was prepared by adding 100 μL of the original suspension of nanoribbons over 1 mL of Milli-Q water. 15 μL of the diluted

suspension were deposited on SiO_2 substrates by drop casting and allowed to adsorb for 15 min at room temperature. The remaining suspension was removed blowing with an Argon flow.

The X-ray diffraction data collection and structure determination for compound **1** was done at 296 K on a Bruker Kappa Apex II diffractometer with graphite-monochromated Mo Kα radiation (λ = 0.71073 Å). The cell parameters were determined and refined by a least-squares fit of all reflections. A semi-empirical absorption correction (SADABS) was applied. All the structures were solved by direct methods using the SIR92 program[2] and refined by full-matrix least-squares on F^2 including all reflections (SHELXL97).[3] During the crystal structure solution it became evident that the thymine residues were disordered. All the attempts to solve the crystal structure using lower symmetry space groups did not avoid the presence of this disorder. The disorder was modelled placing the thymine residues placed over two positions related by a rotation of 180º. The atoms belonging to the disordered part were kept isotropic and soft "SADI" restraints were fixed in order to ensure that the bond distances in both parts of the disordered thymine residues are similar. The hydrogen atoms were included in their calculated positions and refined riding on the respective carbon atoms. All calculations were performed using the WINGX crystallographic software package.[4] Details of the structure determination and refinement are summarized in Table S1.

Synthesis of $[Cu(TAcO)_2(4,4'\text{-bipy})(H_2O)]_n \cdot 2H_2O$ (1)

Method A: A mixture of $Cu(NO_3)_2 \cdot 3H_2O$ (100 mg, 0.41 mmol), TAcOH (152 mg, 0.82 mmol), NaOH (33 mg, 0.82 mmol) and 4,4'-bipy (65 mg, 0.41 mmol) was stirred in 18 mL of water (pH = 6.1) until complete dissolution. Immediately after, a blue solid was formed and the resulting suspension stirred for 1 h at 25 ºC. Then the suspension was filtered off, washed with water, ethanol, diethyl ether and dried in air (200 mg, 76.2 % yield based on Cu). Anal. Calcd. (found) for $C_{24}H_{28}CuN_6O_{11}$ (**1**): C, 45.04 (45.10); H, 4.41 (4.26); N, 13.13 (13.08) and IR selected data (KBr, cm^{-1}): 3521 (s), 3059 (s), 1689 (s), 1610 (s), 1470 (w), 1419 (m), 1358 (w), 1302 (w), 1245 (w), 1230 (w), 1077 (w), 1015 (w), 971 (w), 831 (w).

Method B: A mixture of $Cu(NO_3)_2 \cdot 3H_2O$ (100 mg, 0.41 mmol), TAcOH (152 mg, 0.82 mmol) and 4,4'-bipy (64 mg, 0.41 mmol) was stirred in 18 mL of water (pH = 4.8) for 10 min at 25 ºC. Then the resulting deep blue solution was sealed in a 23 mL Teflon-lined steel autoclave and heated at 140 ºC for 3 days, then cooled to 30 ºC for *ca*. 24 h (*ca*. 0.1

ºC/min). The blue crystals were filtered off, washed with water, ethanol, and diethyl ether and dried in air (110 mg, 41.9 % yield based on Cu). Anal. Calcd. (found) for $C_{24}H_{28}CuN_6O_{11}$ (**1**): C, 45.04 (45.35); H, 4.41 (4.36); N, 13.13 (13.13). IR selected data (KBr, cm^{-1}): 3446 (s), 1704 (s), 1677 (s), 1612 (s), 1471 (w), 1419 (m), 1355 (w), 1301 (w), 1247 (w), 1230 (w), 1078 (w), 1012 (w), 971 (w), 831 (w).

X-ray powder diffraction of both solids and blue crystals samples of compound **1** confirm that crystals and powders are the same compound.

Synthesis of $[Cu(TAcO)_2(4,4'\text{-bipy})(H_2O)]_n \cdot 2H_2O$ Nanoribbons (1n)

A mixture of TAcOH (18 mg, 0.1 mmol) in 1 mL of water and NaOH (3.9 mg, 0.1 mmol) in 1 mL of water was added to a water solution (1 mL) of 4,4'-bipy (7.8 mg, 0.05 mmol) under stirring at 25 ºC. The resulting clear solution turned onto a deep blue colloid upon addition of 1 mL of a water solution of $Cu(NO_3)_2 \cdot 3H_2O$ (1.2 mg, 0.05 mmol). The blue colloid was stirred for 5 min, centrifuged for 5 min at 10000 rpm and washed four times with 4 mL of Milli-Q water. The solid was dried in air (25 mg, 39 % yield based on Cu). Anal. Calcd. (found) for $C_{24}H_{28}CuN_6O_{11}$ (**1**): C, 45.04 (45.17); H, 4.41 (4.26); N, 13.13 (13.08) and IR selected data (KBr, cm^{-1}): 3523 (s), 3450 (s), 1693(m), 1681 (w), 1607 (m), 1612 (s), 1471 (w), 1419 (m), 1355 (w), 1301 (w), 1249 (w), 1230 (w), 1078 (w), 1010 (w), 971 (w), 831 (w), 770 (w). X-ray powder diffraction confirm the structure.

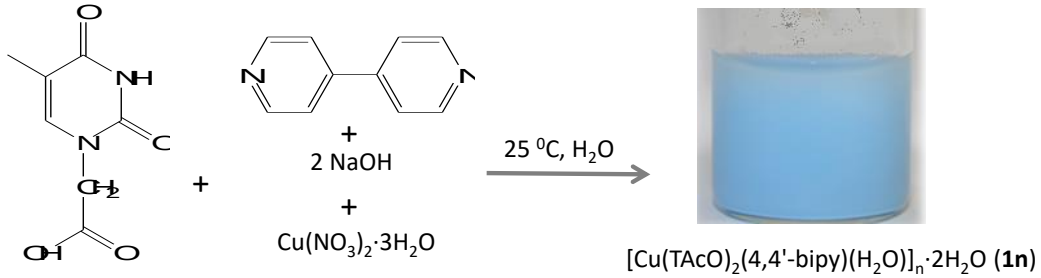

Scheme S1. Illustration of the synthesis of $[Cu(TAcO)_2(4,4'\text{-bipy})(H_2O)]_n \cdot 2H_2O$ (**1n**) as a blue colloid.

S2. X-ray Diffraction Studies

Table S1. Crystallographic data and structure refinement details of compound **1**.[a]

formula	$C_{24}H_{28}CuN_6O_{11}$	V (Å^3)	2697.46(9)
MW (g mol^{-1})	640.06	Z	4
crystal system	monoclinic	ρ_{calcd} (g cm^{-3})	1.576
space group	$P2_1/n$	μ (mm^{-1})	0.882
a (Å)	6.5300(1)	reflections collected	44331
b (Å)	22.2196(5)	unique data/parameters	4883/365
c (Å)	18.7306(4)	R_{int}	0.0414
α (º)	90	Goodness of fit (S)[b]	1.152
β (º)	96.996(1)	R_1[c]/wR_2[d] [I>2σ(I)]	0.0693/0.1941
γ (º)	90	R_1[c]/wR_2[d] [all data]	0.0888/0.2008

[a] Reported data do not include the variable amount of solvent molecules present in the channels. [b]$S = [\sum w(F_0^2 - F_c^2)^2 / (N_{obs} - N_{param})]^{1/2}$; [c]$R1 = \sum||F_0|-|F_c|| / \sum|F_0|$; [d]$wR2 = [\sum w(F_0^2 - F_c^2)^2 / \sum wF_0^2]^{1/2}$; $w = 1/[\sigma^2(F_0^2) + (aP)^2 + bP]$ where $P = (\max(F_0^2,0) + 2Fc^2)/3$ with a = 0.0545 and b = 21.7714.

Table S2. Selected bond lengths (Å) and angles (º) for compound **1**.

Cu1-N31	2.005(6)	N31-Cu1-N41	171.13(17)	N41-Cu1-O291	88.02(18)
Cu1-N41	2.008(6)	N31-Cu1-O191	91.01(18)	N41-Cu1-O1w	94.7(2)
Cu1-O191	1.970(3)	N31-Cu1-O291	88.87(19)	O191-Cu1-O291	172.40(14)
Cu1-O291	2.020(4)	N31-Cu1-O1w	94.1(2)	O191-Cu1-O1w	88.14(15)
Cu1-O1w	2.307(5)	N41-Cu1-O191	90.98(18)	O291-Cu1- O1w	99.45(15)

Table S3. Hydrogen bonding interactions (Å, º) in compound **1**.[a]

D–H···A[b]	H···A	D···A	D–H···A
O1w–H···O192^{i}	2.02	2.844(6)	162.5
O1w–H···O292	1.98	2.702(6)	141.7
O2wA–H···O192^{ii}	2.05	2.893(11)	171.3
O2wA–H···O191^{iii}	2.03	2.877(11)	170.6
O2wB–H···O292^{iv}	1.94	2.791(10)	170.9
O2wB–H···O291^{v}	2.03	2.877(10)	171.1
O3wA–H···O292^{vi}	1.98	2.825(10)	170.4
O3wA–H···O291^{vii}	2.02	2.865(10)	170.5
O3wB–H···O192^{viii}	2.04	2.890(10)	165.7
O3wB–H···O191^{ix}	2.00	2.842(10)	175.7
C33-H···O24A^{vi}	2.46	3.376(11)	168.2
C33-H···O24B^{vi}	2.24	3.161(10)	170.3
C35-H···O14A^{ii}	2.39	3.312(11)	169.0
C35-H···O14B^{ii}	2.18	3.103(9)	170.7
C43-H···O14A^{viii}	2.26	3.180(10)	171.1
C43-H···O14B^{viii}	2.41	3.342(10)	175.5
C45-H···O24A^{iv}	2.21	3.130(10)	170.6
C45-H···O24B^{iv}	2.37	3.299(11)	178.4
C16A-H···O12B^{ix}	2.34	3.195(14)	152.8
C16B-H···O12B^{vii}	2.32	3.178(15)	153.4
C26A-H···O22B^{v}	2.34	3.196(15)	153.6
C26B-H···O22A^{iii}	2.31	3.165(15)	152.9

[a]Symmetry codes: (i) x-1, y, z; (ii) x-3/2, -y+1/2, z-1/2; (iii) x-1/2, -y+1/2, z-1/2; (iv) –x, -y+1, -z; (v) –x+1, -y+1, -z; (vi) x+3/2, -y+1/2, z+1/2; (vii) x+1/2, -y+1/2, z+1/2; (viii) –x+3, -y+1, -z+1; (ix) –x+2, -y+1, -z+1.

The supramolecular structure of **1** is sustained by a complex network of hydrogen bonds (Figure S1, Table S3). The stronger hydrogen bonds involve the water molecules as a donor of hydrogen bonds to the carboxylate oxygen atoms and as acceptor from the thymine N3-H position. There are also C-H···O hydrogen bonds involving the aromatic C-H positions of the 4,4´-bipyridine bridging ligand and thymine residue as donors and the thymine ketone groups as acceptors. It is worth to note that there are no base pairing interactions between the thymine residues probably due to the presence of water molecules that disrupt these interactions. There is no evidence of π-π stacking interactions.

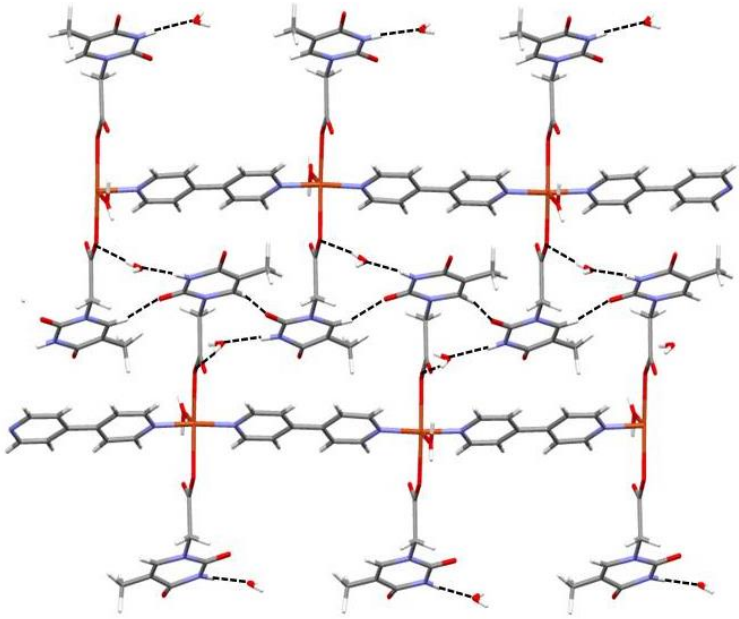

Figure S1. Supramolecular 3D structure formed by a complex network of hydrogen bonds.

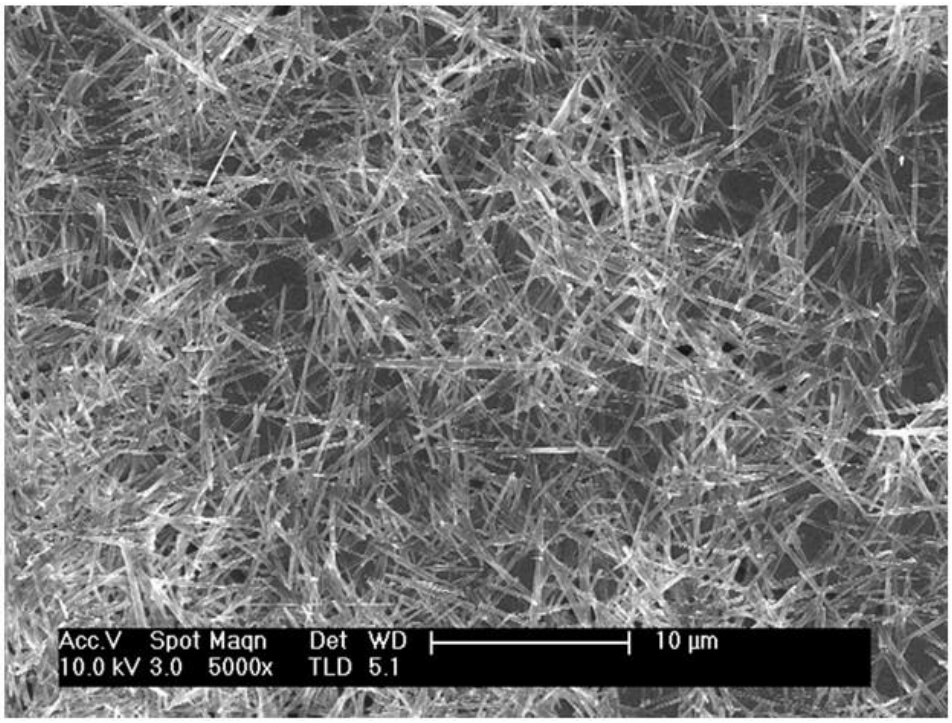

Figure S2. FESEM image of a freshly prepared **1n** sample showing the homogeneity of the sample.

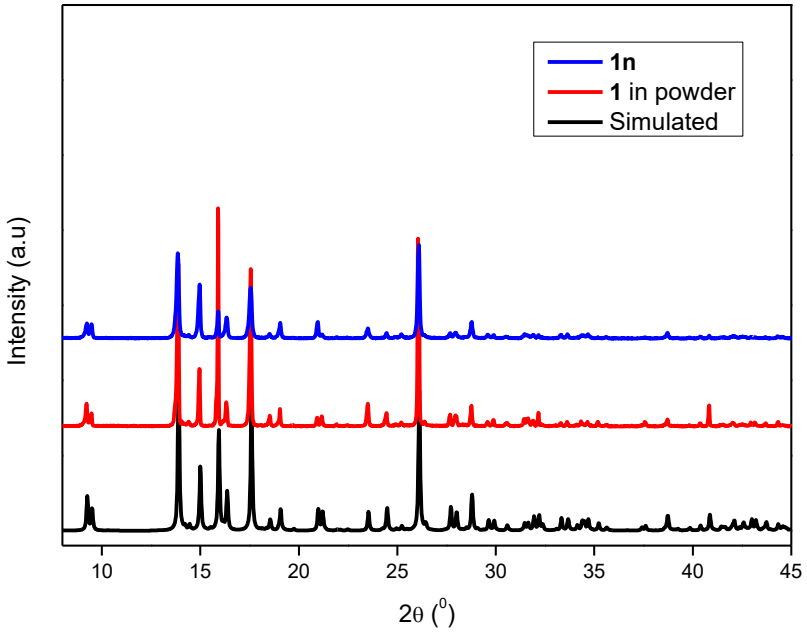

Figure S3. X-ray powder diffraction patterns of simulated from DRX data from the single crystal structural elucidation of compound **1** (black line), microcrystalline compound **1** in solid (red line) and **1n** nanoribbons (blue line).

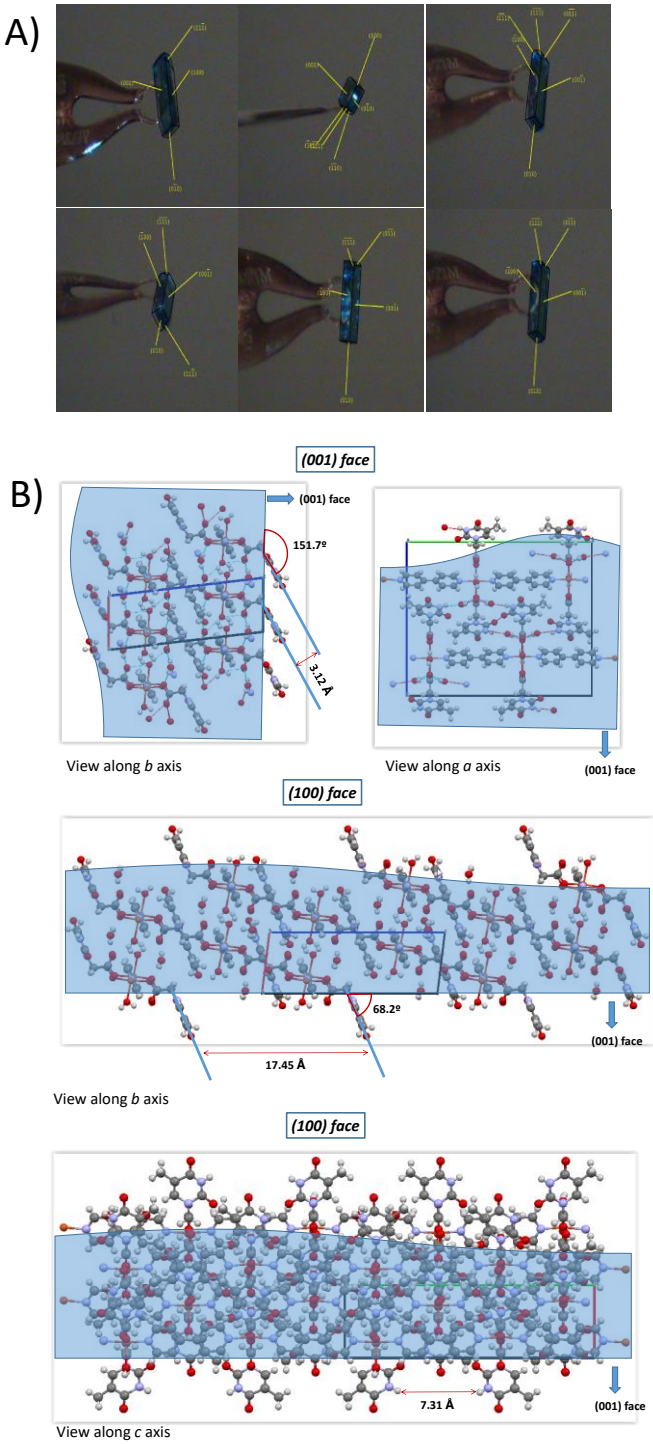

Scheme S2. A) Several pictures of a monocrystal of **1** showing the indentation of the faces; B) Disposition of the thymine residue along different crystallographic planes of the crystal of compound **1**. The sides of the crystal (which are the largest) expose the thymine. While the front face (010) does not, as coincides with the direction of propagation of the chain. In summary the findings, strengthen our hypothesis that the interaction of adenine, with thymine residues that form the developed faces of these crystals.

S3. Studies on the effect in the morphology of *1n* prepared under different experimental conditions preparation or storage at different times and pHs.

S3.1 Effect of the concentration of the reactants in *1n* morphology.

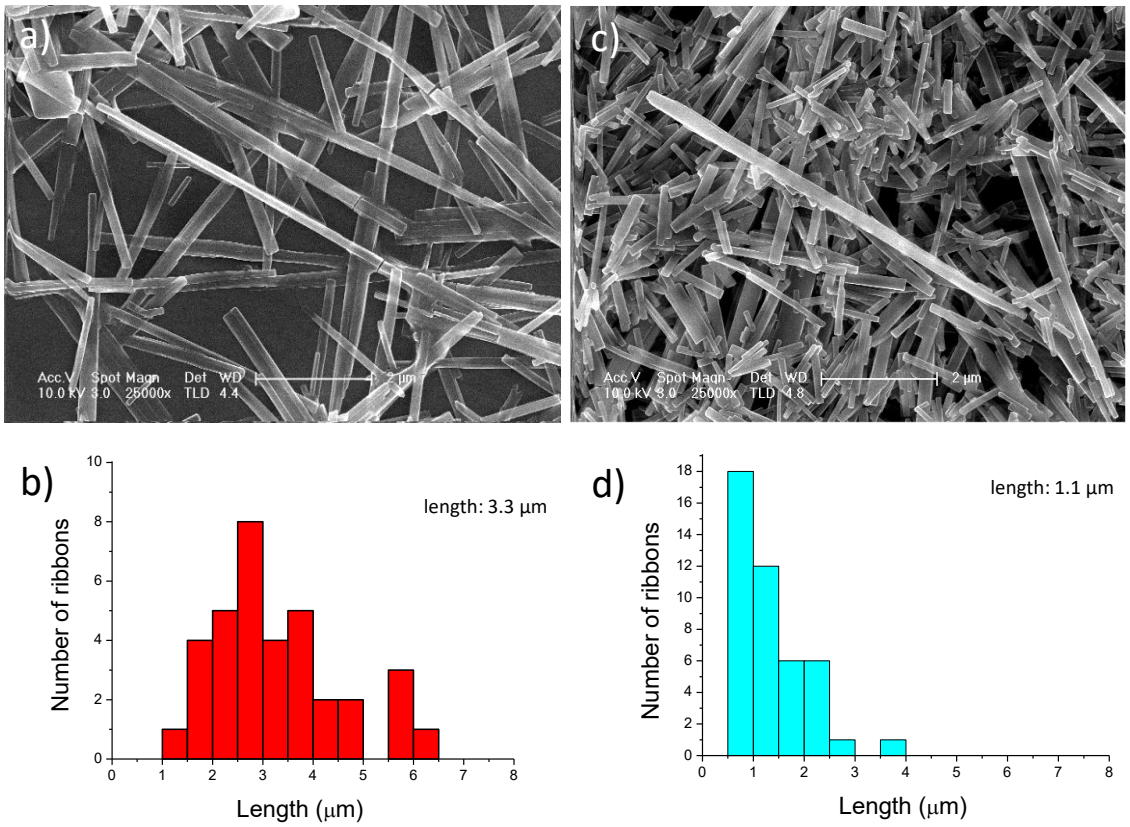

Figure S4. FESEM images and corresponding size-distribution histograms of (**a,b**) a freshly prepared **1n** sample, following the standard synthetic procedure for **1n** preparation (pH 6.1 and 0.05 M), and (**c,d**) at a higher concentration, 0.2 M.

S3.2 Effect of the pH values in *1n* morphology.

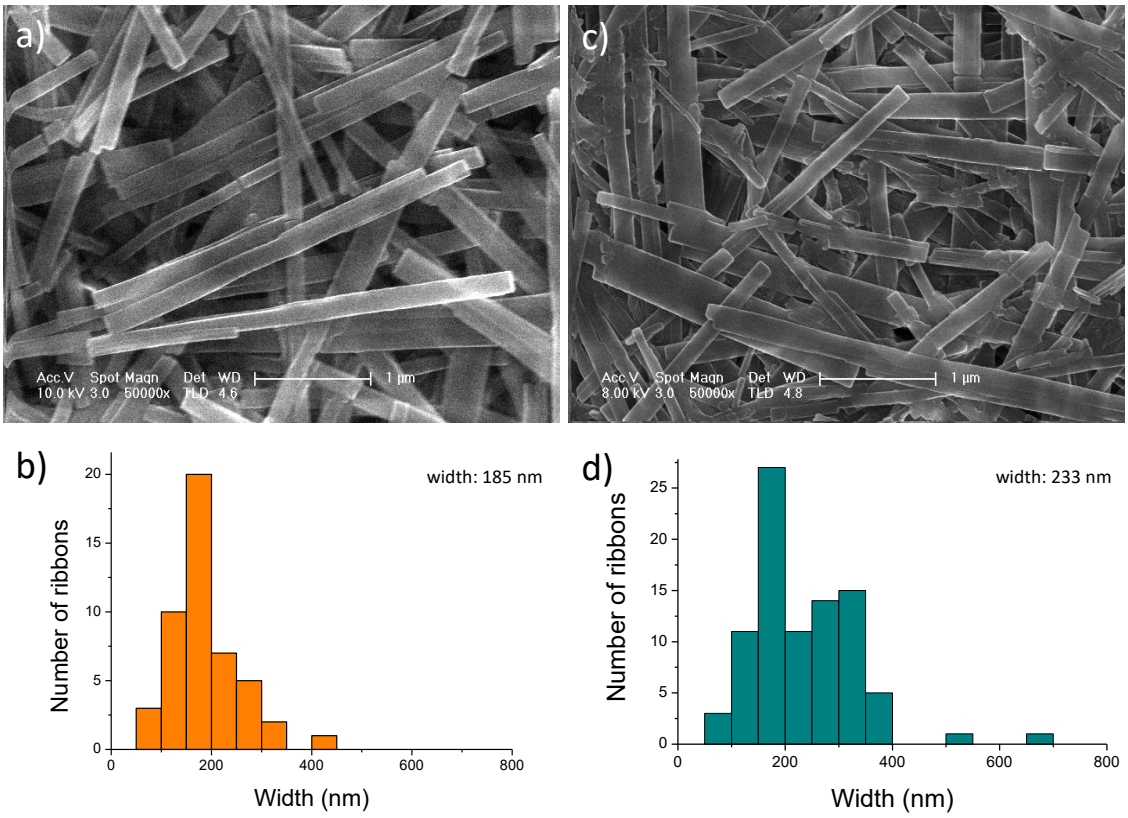

Figure S5. FESEM images and corresponding histograms of a freshly prepared **1n** sample, following the standard synthetic procedure for **1n** preparation (pH 6.1 and 0.05 M) (**a**,**b**) and a sample prepared at a 0.05 M and pH 7.4 (pH adjusted upon addition of NaOH 0.1 M) (**c**,**d**).

S3.3 Effect of the time storage in *1n* morphology.

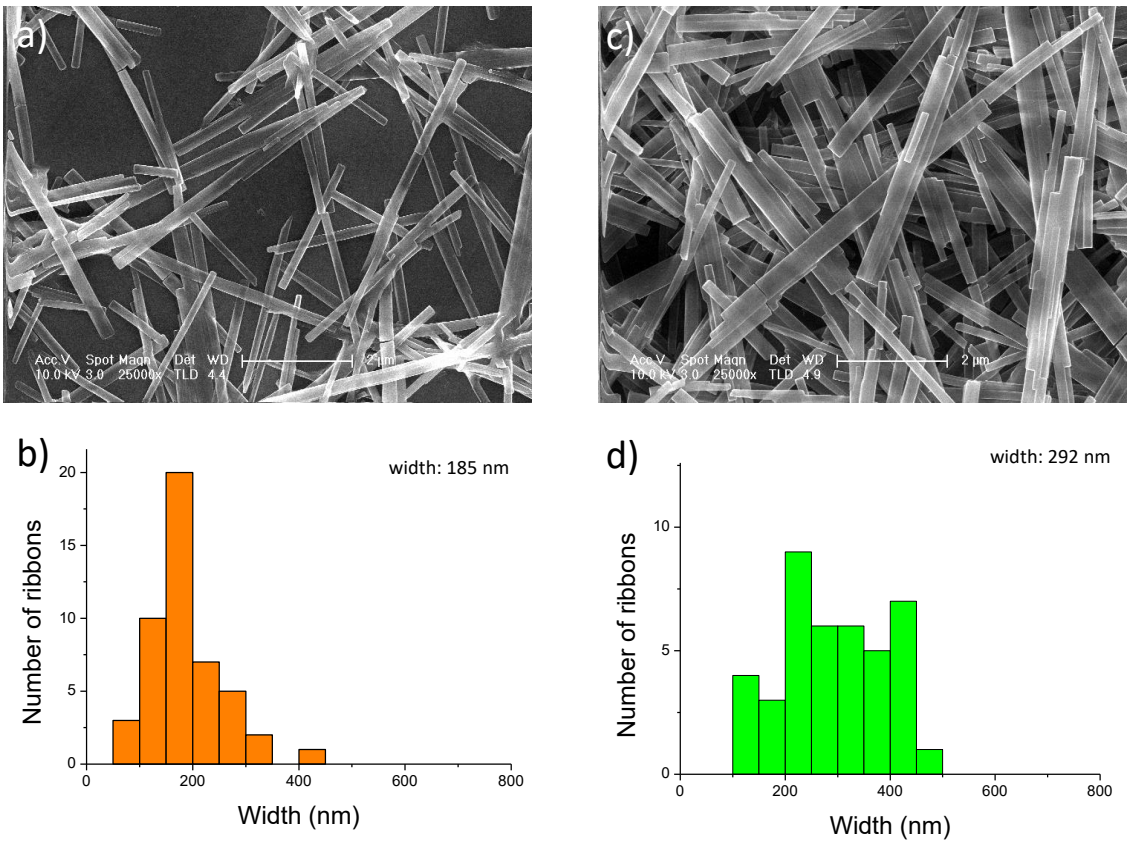

Figure S6. FESEM images and corresponding histograms of (**a**,**b**) a freshly prepared **1n** sample, following the standard synthetic procedure for **1n** preparation (pH 6.1 and 0.05 M) and (**c**,**d**) an aged **1n** colloid (stored for 1 month at 25 ºC and pH 6.1).

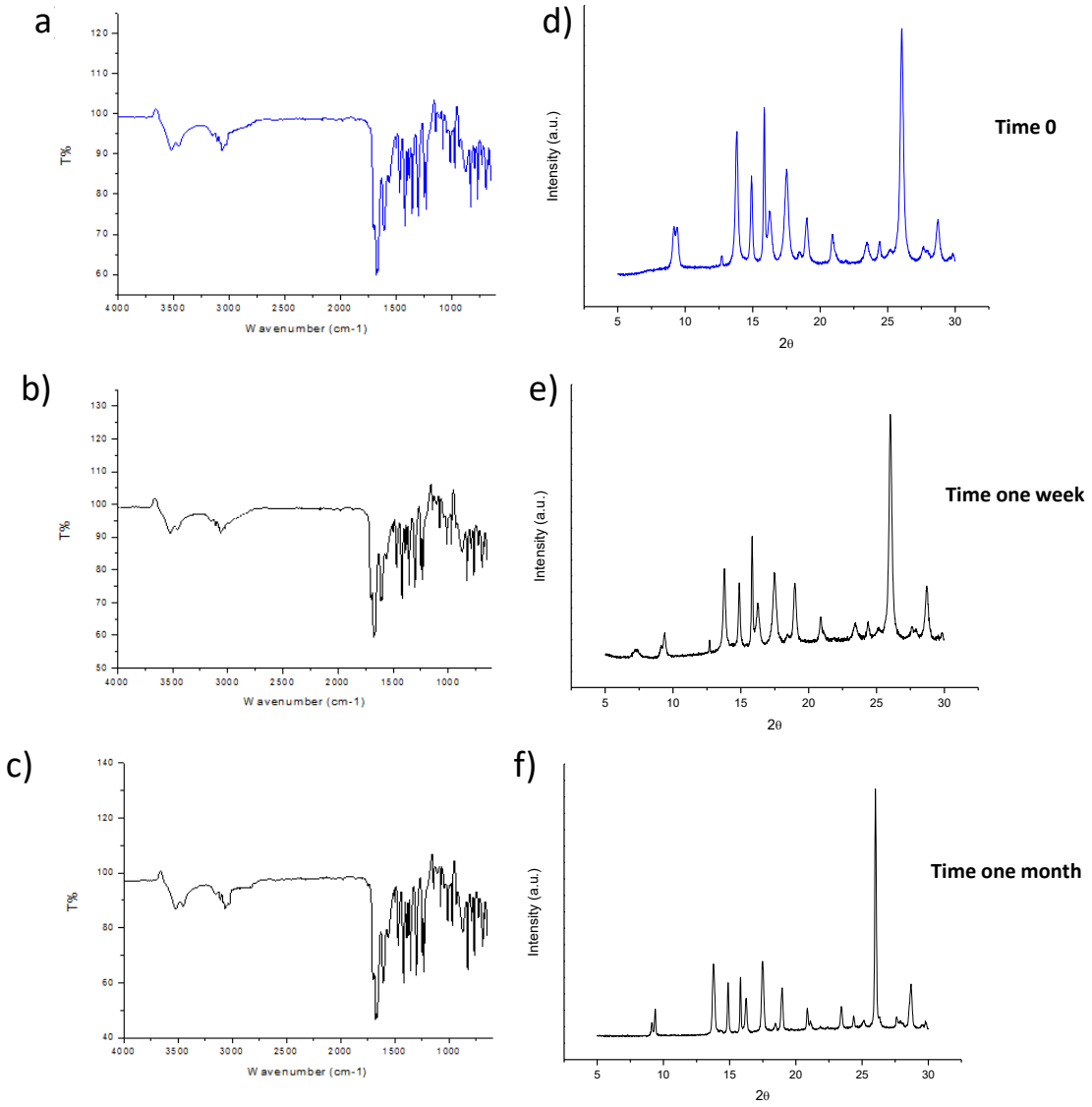

Figure S7. FTIR and X-ray powder diffraction data of a freshly prepared **1n** (a,d), an aged **1n** colloid (stored for 1 week at 25 ºC and pH 6.1; b,e), and an aged **1n** colloid (stored for 1 month at 25 ºC and pH 6.1; c,f).

S4. Biological Assays

S4.1 Modified Oligonucleotide Synthesis

The oligonucleotides (Entries 1-4, Table S4) were prepared using a MerMade4 DNA Synthesizer using commercial phosphoramidites (Link Technologies). After solid-phase synthesis, the solid support was transferred to a screw-cap glass vial and incubated at 55 ºC for 4 h with 2 mL of ammonia solution (33 %). After the vial was cooled on ice the supernatant was transferred by pipet to microcentrifuge tubes and the solid support and the vial were rinsed with water. The combined solutions were evaporated to dryness using an evaporating centrifuge.

The samples were purified by polyacrylamide gel electrophoresis 20 % and the oligonucleotides were eluted from gel fractions using an elutrap system. The solutions were desalted using a NAP-10 column and concentrated in an evaporating centrifuge.

Oligonucleotides represented in the entries 5-7 (Table S4) were purchased from IDT.

Table S4. Deoxynucleotide structures employed in this work. Additionally, PolyA and PolyT labeled with fluorescein were used in the fluorescence studies.

Entry	Name	Sequence
1	PolyA	5’-AAAAAAAAAA-3’
2	PolyC	5’-CCCCCCCCCC-3’
3	PolyG	5’-GGGGGGGGGG-3’
4	PolyT	5’-TTTTTTTTTT-3’
5	SCR	5'-TCGTAAGCAT -3'
6	Duplex	5’-GGACCACCGCATCTCTACATT-(Fluorescein)-3’ 3’-TTCCTGGTGGCGTAGAGATGT
7	Duplex-PolyA	5’-GGACCACCGCATCTCTACATTAAAAAAAAAA-(Fluorescein)-3’ 3’-TTCCTGGTGGCGTAGAGATGT

Duplex formation. The DNA duplexes were obtained by mixing in equal proportions each complementary sequence in the annealing buffer 3× (300 mM potassium acetate, 90 mM HEPES-KOH and 6 mM magnesium acetate). The final concentration of DNA duplexes was 380 μM. The process was carried out in a thermocycler by heating the solutions 5 minutes at 95 °C, and cooling them down to room temperature slowly (5 °C/minute).

S4.2 Affinity Studies

The hydrolysis of nanofibers of $[Cu(TAcO)_2(4,4'\text{-bipy})_2(H_2O)]_n$ (**1n**) have been evaluated with the time (from freshly prepared to 1 week) measuring by ICP-mass spectroscopy the amount of copper ions present in the filtered water solutions of **1n** prepared under the same experimental conditions to that used in the experiments with the oligonucleotides. The results show that **1n** does not undergo any hydrolysis at the time bellow 1h (copper concentration *ca*. 0.6×10^{-6} g/L). After 1h in suspension the amount of copper increases to *ca*. 3×10^{-3} g/L. Longer times (from 2 h up to 1 week) in suspension does not produce any change in the copper concentration detected in solution (*ca*. 3×10^{-3} g/L). Therefore we conclude that the as far as the low concentration of copper in solution remains stable it should not interfere much, or in any case equally to all samples, to the affinity studies of **1n** carried out with oligonucleotides.

The oligonucleotides (5.5 mM) were incubated with **1n** (11 mM) for 2 h at room temperature in 0.600 mL of ultrapure water. Then, the mixture was centrifuged using standard dialysis centrifugal filters (Amicon 10 K, 0.5 mL) to remove the unbound material.

The interaction between **1n** and the oligonucleotides was monitored by absorbance measurements at 260 nm of the mixture just upon mixing the two fractions obtained after dialysis filtration. The absorbance was recorded in a Synergy H4 microplate reader, using a 96 well plate at room temperature.

S4.3 Cell Viability Assay

The cytotoxicity of **1n** was evaluated in C918, Panc-1 and HaCaT cell lines using the resazurin assay C918 cells were seeded onto 24-well plates at a density of 1.5×10^4 cells/well in supplemented RPMI medium (10 % Fetal Bovine Serum (FBS), 1 % L-Glutamine and 1 % Streptomycin/Penicillin). Panc-1 and HaCaT cells were seeded onto 24-well plates at a density of 2×10^4 cells/well in supplemented DMEM medium (10 % FBS, 1 % L-Glutamine and 1 % Streptomycin/Penicillin). Then, cells were incubated at standard conditions (37 °C, 5 % CO_2) for 16 h, and the medium was replaced with fresh culture medium containing 1, 50, 100, 150 and 200 μM of **1n**. After 24 h of incubation, cells were washed twice with PBS, and incubated 48 h more. Then, the medium was

replaced by fresh medium containing 1 % of a resazurin reagent solution (1 mg/mL of resazurin in PBS pH = 7.4). Cells were incubated for 3 h and the fluorescence was measured (Excitation = 550 nm, Emission = 590 nm) using a Synergy H4plate reader. Cytotoxicity was expressed as a percentage of the control. All the experiments were performed in triplicate and the standard deviation is represented in the error bars.

S4.4 Fluorescent Microscopy Studies

The sample **1n** containing a FITC-labelled oligonucleotide was prepared by the procedure describe before. C918 cells were seeded in a Cell Culture Slide (4 wells) at a density of $1x10^4$ cells/well in supplemented RPMI medium (10 % FBS, 1% L-Glutamine and 1% Penicillin-Streptomycin), and incubated overnight at standard condition (37 °C, 5 % CO_2). Then the medium was replaced with serum-free medium (OptiMem) containing 150 μM of **1n** with 12.5 μM of labeled oligonucleotides (PolyA or PolyT) or 35 μM of labeled DNA duplexes. After 3 h of incubation, cells were washed twice with PBS, and analysed in the microscope (LEICA DMI3000 B).

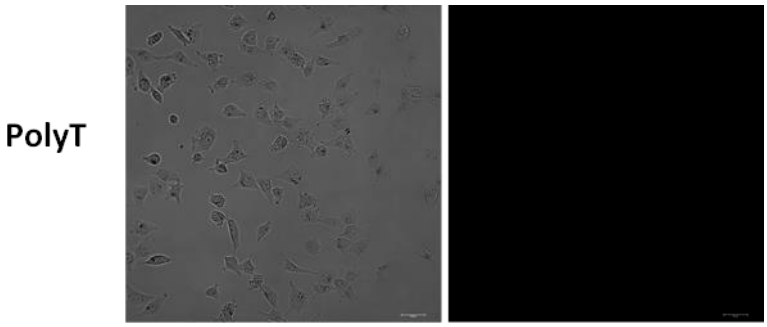

Figure S8. C918 cells incubated with **1n** treated with PolyT labeled with fluorescein. The fluorescence could not be detected, as in Figure 4 of the manuscript.

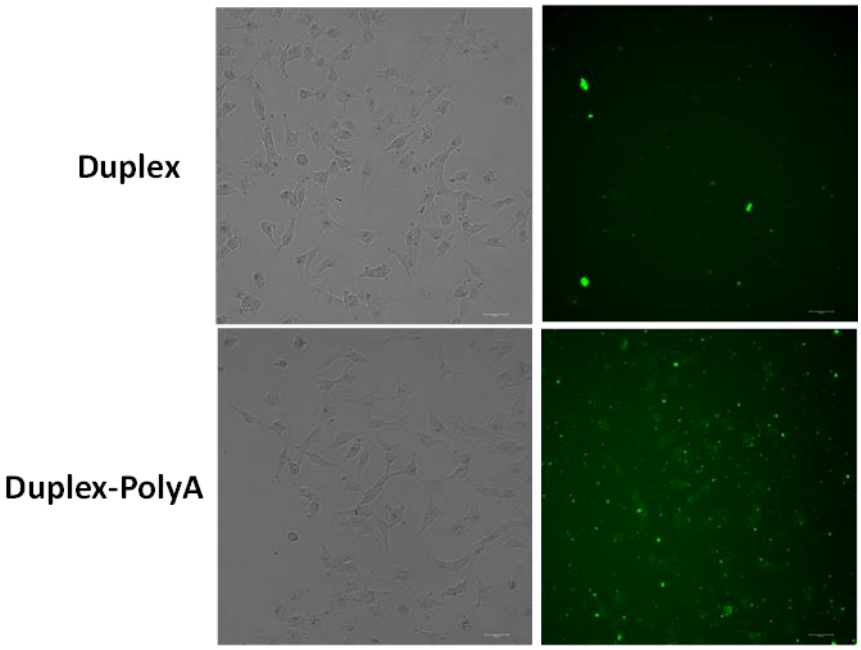

Figure S9. (Up) C918 cells incubated with **1n** treated with a DNA duplex labeled with fluorescein. (Bottom) C918 cells incubated with **1n** treated with a DNA duplex labeled with fluorescein bearing a PolyA tail.

S4.4 Fluorescent Quantification Studies

The fluorescence of the cells was quantified after trypsinization of cells (37 ºC, 2 min). Harvested cells were centrifuged (5 min, 0.4 rcf) and resuspended in 100 µL of PBS, and the fluorescence was measured (Ex 470 nm, Em 530 nm) using a SynergyH4 microplate reader.

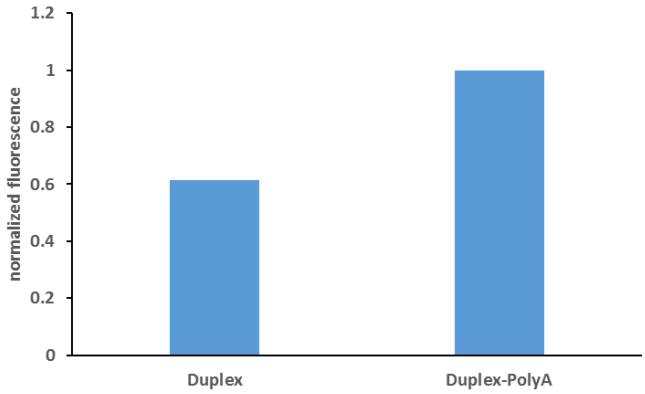

Figure S10. The fluorescence observed in the previous experiment (Figure S9) was quantified. The fluorescence observed when a DNA duplex contains a PolyA tail is 40% higher the one observed with a DNA duplex.

References

[1] G. A. Bain, J. F. Berry, *J. Chem. Edu.* **2008**, *85*, 532.

[2] A. C. Altomare, M.; Giacovazzo, C.; Guagliardi, A., *J. Appl. Crystallogr.* **1993**, *26*.

[3] G. M. Sheldrick, *SHELXL-97, Program for Crystal Structure Refinement; Universität Göttingen.* **1997.**

[4] M. J. Prakash, M. S. Lah, *Chem. Commun.* **2009**, 3326.